Modulational instability of nonlinear spin waves in an atomic chain of spinor Bose-Einstein condensates

Xing-Dong Zhao,[1] ZhengWei Xie,[1,2] and Weiping Zhang[1,*]

[1]*State Key Laboratory of Precision Spectroscopy, Department of Physics, East China Normal University, Shanghai 200062, People's Republic of China*

[2]*College of Physics and Electronic Engineering, Sichuan Normal University, Chengdu 610066, People's Republic of China*

(Received 27 June 2007; published 14 December 2007)

The modulational instability of coherently excited spin waves is studied in an atomic spin chain of spinor Bose-Einstein condensates (BECs) confined in an optical lattice. We examine the dependence of the stability on the long-range nonlinear interaction of spin waves excited at different lattice sites. The long-range nonlinear spin coupling in the optical lattice is due to light-induced and static magnetic dipole-dipole interaction between atoms. We compare the spin wave dynamics in an atomic spin chain of spinor BECs formed in an optical lattice with that in a Heisenberg-like spin chain in solid-state physics. This reveals the important differences of the spin chain with long-range spin coupling from that with the short-range one.

DOI: 10.1103/PhysRevB.76.214408 PACS number(s): 03.75.Mn, 03.75.Kk, 05.30.Jp, 32.80.Lg

I. INTRODUCTION

The experimental observations of spin domains, quantum tunneling across the spin domains, and spin exchange dynamics have led to rapidly growing interest in dynamical properties of Bose-Einstein condensates (BECs) with spin degrees of freedom in the optical trap.[1–4] Among them, the modulational instability (MI) of spinor BECs in a single optical trap has attracted much attention as MI is an indispensable mechanism for understanding a diversity of dynamic processes in the Bose condensed systems such as pattern formation, domain walls, nonlinear spin excitations, quantum phase transition, etc.[1,5–9] Meanwhile, the dynamical properties of spinor BECs in the optical lattices have also been the attracting topics in the blossoming area of ultracold atoms. A number of phenomena including the spin mixing, spin textures, spontaneous magnetization, spin waves, macroscopical spin tunneling have been studied.[5,6,10,11] On the other hand, the spinor BECs in the optical lattices provide a unique tool to study the analog of spin quantum dynamics of Bose systems to that of electrons in condensed matter physics.[12–16] In this paper, we develop a study on the MI of extended nonlinear spin waves of spinor BECs in the optical lattice. From the condensed matter physics, we have learnt that the MI of extended nonlinear spin waves in solid-state systems of spin chains has been an important process affecting the spin-related properties of magnetic materials.[15–20] In the solid-state spin systems, the MI of extended nonlinear spin waves mainly originates from the Heisenberg-like short-range exchange interaction between electrons. The theoretical models and treatment are limited to only the approximation of nearest-neighbor interaction. All long-range interactions are neglected. In our knowledge, the MI of extended nonlinear spin waves in lattice spin systems, where the long-range interaction between different spin sites is dominant, has not yet been explored so far.

In our previous work, we have shown that one-dimensional optical lattice can be used to confine spinor BECs to form a coherent atomic spin chain.[10,11,21] In this case, the spinor BECs behave like spin magnets and can interact with each other through both the light-induced dipole-dipole interaction and the static magnetic dipole-dipole interaction. As a result, an analogy of atomic chains of spinor BECs can be made to the spin chains in the solid-state magnetic systems. However, a key difference of the atomic spin chain from solid-state one is that we are facing a completely new spin system in atomic physics where the long-range interactions play a dominant role in the spin dynamics. This paper is organized as follows. In Sec. II, we establish a physical model to describe the coherent atomic spin chain containing spinor BECs which are confined in an optical lattice and subject to the long-range dipole-dipole interaction. In Sec. III, we start from an atomic spin chain where the excitations of nonlinear coherent spin waves (NCSWs) exist.[10] In this case, using the Holstein-Primakoff transformation and the method of linear stability analysis,[7,8,15] we study the MI of the extended NCSWs with the long-range site-to-site spin coupling through the dipole-dipole interaction. The explicit expressions of the stability criteria for the extended NCSWs are established in general. For detailed study, we focus on the NCSW modes near the Brillouin zone boundary with the long wavelength modulational instability. In order to determine the role of long-range site-to-site spin coupling in the spin dynamics in the optical lattice, we compare the behaviors of the spin wave MI for the different cases of the nearest-neighbor (NN) approximation, the next-nearest-neighbor (NNN) approximation, and the long-range spin coupling, respectively. In Sec. IV, we carry out the detailed numerical simulations for the MI of the extended NCSWs in the time evolution. The conclusions are given in Sec. V.

II. HAMILTONIAN OF SPINOR BOSE-EINSTEIN CONDENSATE IN THE OPTICAL LATTICE

We consider a one-dimensional optical lattice formed by two π-polarized laser beams counterpropagating along the y axis. The two lattice laser beams are detuned far from atomic resonance, and the condensate confined in the lattice is approximately in its electronic ground state. We assume that

the lattice potential is deep enough so that the condensate is divided into a set of separated small condensates located at each lattice sites.[10] For $F=1$ spinor condensates, the individual condensates consist of atoms with three Zeeman magnetic sublevels; hence, they behave as collective spin magnets in the presence of external magnetic fields. Such spin magnets form a one-dimensional (1D) coherent atomic spin chain along the optical lattice. Under the tight-binding approximation and ignoring both the nonresonant and spin-independent constant terms, the $F=1$ spinor BEC in the optical lattices can be described in terms of the following spin Hamiltonian:[10]

$$H=\sum_i\left[\lambda_a'\hat{\mathbf{S}}_i^2-\gamma_B\hat{\mathbf{S}}_i\cdot\mathbf{B}-\sum_{j\neq i}J_{ij}^z\hat{S}_i^z\hat{S}_j^z-\sum_{j\neq i}J_{ij}(\hat{S}_i^-\hat{S}_j^+ + \hat{S}_i^+\hat{S}_j^-)\right], \tag{1}$$

where $\hat{\mathbf{S}}_i$ is the ith collective spin operator, with components $\hat{S}_i^{\{\pm,z\}}$. The first term in the Hamiltonian results from the spin-dependent interatomic collisions at a given lattice site, with $\lambda_a'=(1/2)\lambda_a\int d^3\mathbf{r}|\phi_i(\mathbf{r})|^4$. The $\mathbf{B}$ is an external magnetic field oriented along the z axis, leading to the second term of Zeeman energy. The parameter $\gamma_B=-\mu_B g_F$ is the gyromagnetic ratio with g_F being the Landé g factor and μ_B the Bohr magneton. The external magnetic field $\mathbf{B}$ is strong enough to polarize the ground-state spin orientations of the atomic chain along the quantization axis z.[11] The last two terms describe the site-to-site spin coupling induced by both the static magnetic dipole-dipole interaction and the light-induced dipole-dipole interactions. The coupling coefficients have the following forms:[10]

$$J_{ij}^z=\frac{\mu_0\gamma_B^2}{16\pi\hbar^2}\int d\mathbf{r}\int d\mathbf{r}'\frac{|\mathbf{r}'|^2-3y'^2}{|\mathbf{r}'|^5}|\phi_i(\mathbf{r})|^2|\phi_j(\mathbf{r}-\mathbf{r}')|^2, \tag{2}$$

$$J_{ij}=\frac{U_0}{144\hbar^2k_L^3}\int d\mathbf{r}\int d\mathbf{r}'f_c(\mathbf{r}')\exp\left(\frac{\mathbf{r}_\perp^2+|\mathbf{r}_\perp-\mathbf{r}_\perp'|^2}{W_L^2}\right)\times\cos(k_Ly)\cos[k_L(y-y')]\mathbf{e}_{+1}\cdot\mathbf{W}(\mathbf{r}')\cdot\mathbf{e}_{-1}|\phi_i(\mathbf{r})|^2\times|\phi_j(\mathbf{r}-\mathbf{r}')|^2+\frac{1}{2}J_{ij}^z, \tag{3}$$

where a cutoff function $f_c(\mathbf{r})=\exp(-r/L_c)$ has been introduced to describe the effective interaction range of the light-induced dipole-dipole interaction, with L_c being the coherence length associated with different decoherence mechanisms such as the collective spontaneous emission and collective absorption of N atoms.[22] The wave number $k_L=2\pi/\lambda_L$, the transverse coordinate $r_\perp=\sqrt{x^2+z^2}$, and W_L the width of the lattice laser beams. The $\mathbf{e}_{\pm1,0}$ are unit vectors in the spherical harmonic basis. The tensor $\mathbf{W}(\mathbf{r})$ describes the spatial profile of the light-induced dipole-dipole interaction and has the form $\mathbf{W}(\mathbf{r})=\frac{3}{4}[(\mathbf{11}-3\hat{\mathbf{r}}\hat{\mathbf{r}})[\sin(\xi)/\xi^2+\cos(\xi)/\xi^3]-(\mathbf{11}-\hat{\mathbf{r}}\hat{\mathbf{r}})\cos(\xi)/\xi]$, where $\mathbf{11}$ is the unit tensor, $\hat{\mathbf{r}}=\mathbf{r}/|\mathbf{r}|$, and $\xi=k_L|\mathbf{r}|$. The depth of optical lattice potential is defined as $U_0=\hbar|\Omega|^2/6\Delta$, with Ω being the Rabi frequency. From Eqs. (2) and (3), we see that the light-induced dipole-dipole interaction in the presently designed optical lattice leads to the spin coupling only in the transverse direction (the direction perpendicular to the magnetic field). In this sense, the atomic spin chain formed in the optical lattice is anisotropic when the light-induced dipole-dipole interaction exists. On the contrary, the spin coupling induced only by static magnetic dipole-dipole interaction is isotropic.

In this paper, we consider only the ferromagnetic condensates.[11] In the ground state of the ferromagnetic spin chain of atomic Bose condensates described by Hamiltonian (1), the spins of atoms at each lattice site align up along the direction of the applied magnetic field (the quantized z axis). As a result, the Hamiltonian (1) can be bosonized in terms of the well-known Holstein-Primakoff transformation for the spin operator[23]

$$\hat{S}^+=(\sqrt{2S-a^\dagger a})a,\quad \hat{S}^-=a^\dagger(\sqrt{2S-a^\dagger a}),\quad \hat{S}_z=(S-a^\dagger a), \tag{4}$$

where a and $a^\dagger$ are the boson annihilation and creation operators which describe the spin deviation from the quantum z axis. Physically, the spin deviation corresponds to the excitations of spin waves. For a strong applied magnetic field considered in this paper, the spin deviation due to excitations is relatively weak. Hence, we neglect the fourth-order terms in the expansion of $\sqrt{2S-a^\dagger a}$, and the Hamiltonian (1) can be transformed to

$$\begin{aligned}H_s=&\lambda_a'NS(S+1)-\gamma_BB_zNS+\gamma_BB_z\sum_i a_i^\dagger a_i-\sum_i\sum_{j\neq i}J_{ij}^z(S^2\\&-Sa_j^\dagger a_j-Sa_i^\dagger a_i+a_i^\dagger a_ia_j^\dagger a_j)-2\sum_i\sum_{j\neq i}J_{ij}S(a_i^\dagger a_j+a_ia_j^\dagger)\\&+\frac{1}{2}\sum_i\sum_{j\neq i}J_{ij}(a_i^\dagger a_i^\dagger a_ia_j+a_i^\dagger a_j^\dagger a_ja_j+a_ia_j^\dagger a_j^\dagger a_j+a_i^\dagger a_ia_ia_j^\dagger)\\&+\cdots.\end{aligned} \tag{5}$$

The Hamiltonian (5) describes the excitations of nonlinear spin waves in the ferromagnetic spin chain of atomic spinor BECs. Here, we are interested in the coherent excitations of spin in the system: A cluster of spin at each lattice site undergoes a large excursion as compared with the rest of the spins, and a physically acceptable candidate for quantum states of such large-amplitude collective modes may be coherent states.[24] Under the spin-coherent state representation, using the time-dependent variation principle, we can transform the equation of motion of operator a_l into the equation of motion of probability amplitude ψ_l, where $\psi_l=\langle\psi_l|a_l|\psi_l\rangle$ is the probability amplitude describing the NCSW excited at the lattice site l,

$$\begin{aligned}i\frac{\partial\psi_l}{\partial t}=&\gamma_BB_z\psi_l+\sum_j2J_{lj}^zS\psi_l-\sum_j2J_{lj}^z\psi_j^\dagger\psi_j\psi_l-\sum_j4J_{lj}S\psi_j\\&+\sum_jJ_{lj}(2\psi_l^\dagger\psi_l\psi_j+\psi_j^\dagger\psi_j\psi_j+\psi_j^\dagger\psi_l\psi_l).\end{aligned} \tag{6}$$

III. MODULATIONAL INSTABILITY OF NONLINEAR SPIN WAVES IN ATOMIC SPIN CHAIN

A. Modulational instability criterion

Equation (6) governs the nonlinear dynamics of coherently excited spin waves in an optical lattice. For an atomic spin chain formed in an optical lattice, a big advantage over the solid-state spin chain to study nonlinear spin dynamics is that all the physical parameters $\{J_{ij}\}$ are controllable through the external lattice laser beams. For the investigation of the MI of spin waves presented here, we examine the stability of an extended spin excitation, described as a plane wave, in the presence of sufficiently small perturbations. First, we look at the time evolution of a perturbed coherent spin wave of the form

$$\psi_l(t) = [\phi_0 + b_l(t)]\exp i[\theta_l(t) + \varphi_l(t)] = [\phi_0 + b_l + i\phi_0\varphi_l]\exp i[\theta_l], \tag{7}$$

where ϕ_0 is a constant amplitude of a plane spin wave and its phase $\theta_l(t) \equiv ql - \omega_0 t$, and q is the wave number of the coherent spin waves. The amplitude and phase perturbations b_l and φ_l are real and much smaller than those of the spin wave in the magnitude. The frequency ω_0 of spin wave obeying the nonlinear dispersion relation is

$$\omega_0 = \gamma_B B_z + \sum_j 2J_{lj}^z S - \sum_j 2J_{lj}^z \phi_0^2 - \sum_j 4J_{lj} S\cos(qj - ql) + \sum_j 4J_{lj}\phi_0^2 \cos(qj - ql). \tag{8}$$

Since $|b_l(t)| \ll \phi_0$ and $|\varphi_l(t)| \ll \theta_l(t)$, taking into account Eq. (8), we obtain the following linear coupled equations of b_l and φ_l from Eq. (6):

$$\frac{\partial b_l}{\partial t} = \sum_j 4SJ_{lj}\phi_0(\varphi_l - \varphi_j)\cos(qj - ql) - \sum_j 4SJ_{lj}b_j \times \sin(qj - ql) + \sum_j [2J_{lj}\phi_0^3 \cos(qj - ql)(\varphi_j - \varphi_l) + 4J_{lj}\phi_0^2 b_j \sin(qj - ql)], \tag{9}$$

$$-\phi_0\frac{\partial \varphi_l}{\partial t} = -\sum_j 4J_{lj}^z\phi_0^2 b_j - \sum_j 4SJ_{lj}[(b_j - b_l)\cos(qj - ql) - \varphi_j\phi_0 \sin(qj - ql)] + \sum_j J_{lj}[-4\phi_0^3\varphi_j \sin(qj - ql) + (6b_j + 2b_l)\phi_0^2 \cos(qj - ql)]. \tag{10}$$

The properties of the eigensolutions of Eqs. (9) and (10) determine the stability of the extended spin excitations. One exponentially growing amplitude of perturbation with time t in the eigensolutions is the signature of the MI. This can be identified by working out the eigenvalues of Eqs. (9) and (10). For the purpose, we assume

$$\varphi_l = \varphi \exp i(Ql + \Omega t) + \text{c.c.},$$

$$b_l = b \exp i(Ql + \Omega t) + \text{c.c.}, \tag{11}$$

where Q and Ω are the wave number and frequency of the modulation wave, respectively. Substituting Eqs. (11) into Eqs. (9) and (10), we obtain two coupled linear equations,

$$\begin{bmatrix} \Omega - M_{11} & M_{12} \\ M_{21} & \Omega - M_{22} \end{bmatrix}\begin{bmatrix} b \\ \phi_0\varphi \end{bmatrix} = 0, \tag{12}$$

where

$$M_{11} = M_{22} = \sum_j (4J_{lj}\phi_0^2 - 4SJ_{lj})\sin(Qj - Ql)\sin(qj - ql), \tag{13}$$

$$M_{12} = i\sum_j [2J_{lj}\phi_0^2 - 4SJ_{lj}]\cos(qj - ql)[\cos(Qj - Ql) - 1], \tag{14}$$

$$M_{21} = i\sum_j \{[4J_{lj}^z\phi_0^2 + 4SJ_{lj}\cos(qj - ql) - 6J_{lj}\phi_0^2 \times \cos(qj - ql)]\cos(Qj - Ql) - (2J_{lj}\phi_0^2 + 4SJ_{lj}) \times \cos(qj - ql)\}. \tag{15}$$

The condition that Eq. (12) has a nontrivial solution requires its determinant vanishing. This gives the eigenvalues

$$\Omega = M_{11} \pm \sqrt{M_{12}M_{21}}. \tag{16}$$

When the eigenvalue Ω is imaginary ($M_{12}M_{21} < 0$), the perturbation b_l will grow exponentially, and the excited nonlinear spin waves exhibit the MI. As a result, from the value of Ω, we can determine the stable and unstable regions for different modulations. It is obvious that the MI regions depend not only on the wave number of the extended spin wave q and that of the perturbation wave Q but also on the nonlinear spin coupling coefficients J_{lj} and J_{lj}^z. Once the properties of the nonlinear spin coupling are determined, the MI of the spin waves in the optical lattice will be identified through the criteria $M_{12}M_{21} < 0$. In order to quantitatively and analytically identify the MI regions, here we focus our discussions on the NCSW modes near the Brillouin zone boundary with the long wavelength modulational instability ($Q \ll 1$). This is also the case usually adopted in the experiments for solid-state spin systems.

From Eqs. (13)–(16), we have learnt that the nonlinear spin coupling described by the coefficients J_{lj} and J_{lj}^z plays an important role in the nonlinear dynamics of spin waves. Being different from the spin chains in the solid-state systems, the properties of the spin coupling in the lattice atomic spin chain of spinor BECs can be controlled by tuning the lattice laser beams and the shape of the condensate at each lattice site. Such a character makes the lattice atomic spin chain an ideal tool to study a diversity of spin-related phenomena. To have a look at the properties of spin coupling, we examine the dependence of the spin coupling coefficients J_{lj} and J_{lj}^z on the lattice laser parameters and the shape of the

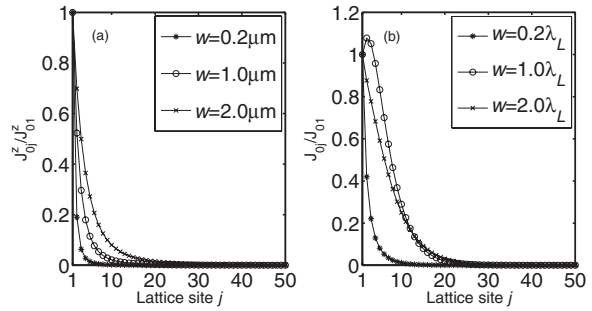

FIG. 1. The static magnetic and the light-induced spin coupling coefficients in the optical lattice as a function of the lattice site index j for different transverse widths of the condensate. The laser parameters are taken as $\lambda_L=1$ μm and $\gamma|\Omega|^2/\Delta^2=10^5$. The gyromagnetic ratio is chosen as $\gamma_B=-\mu_B/2$ of electronic ground state of ^{87}Rb.

condensate including the laser detuning, the laser intensity, and the transverse width of the condensate. The laser detuning Δ classifies the optical lattice into two categories: red-detuned optical lattice ($\Delta<0$) and blue-detuned one ($\Delta>0$). For a blue-detuned lattice, the condensed atoms are trapped at the standing-wave nodes where the laser intensity is approximately zero $[\cos(k_L y)\approx 0]$. As a result, the light-induced dipole-dipole interaction can be neglected. In this case, the spin coupling is governed only by the coefficient J_{ij}^z caused from the static magnetic dipole-dipole interaction. On the contrary, for a red-detuned lattice, the condensed atoms are trapped at the maxima of the intensity of the standing-wave laser and the spin coupling is dominantly determined by the light-induced dipole-dipole interaction. In particular, the spin coupling is anisotropic in this case. For given laser parameters, the spin coupling coefficients, varying with the lattice sites and the transverse width of the condensate, are worked out and displayed in Fig. 1. In the calculation, we consider as an example the $F=1$ electronic ground state ($^3S_{1/2}$) of ^{87}Rb, which has the Landé factor $g_F=-1/2$ and the gyromagnetic ratio $\gamma_B=-\mu_B/2$. In general, the magnetic dipole-dipole interaction depends on the kind of atoms used. For instance, for chromium condensates,[25] which has a larger gyromagnetic ratio $\gamma_B=2\mu_B$, one expects a stronger magnetic dipole-dipole interaction. However, in red-detuned lattices, by controlling the laser parameters, we may always make the light-induced dipole-dipole interaction dominate over the static magnetic dipole-dipole interaction.

For a 1D optical lattice in our case, we have assumed that along the lattice direction (the y direction), the spatial size of the condensate is much less than the lattice wavelength λ_L for the tight-binding confinement, and the condensate has a Gaussian shape with a width w in the transverse x-z plane. From Fig. 1, it is clear that the spin coupling coefficients are sensitive to the variation of the transverse width w of the condensate for both static magnetic and light-induced dipole-dipole interactions. For the static magnetic dipole-dipole interaction shown in Fig. 1(a), the wider the condensate is in the transverse direction, the more important the long-range effect becomes in the spin coupling. The spin coupling induced by light-induced dipole-dipole interaction, in general, exhibits the similar long-range behavior to that by the static magnetic one. However, there is a difference that the light-induced spin coupling has a preference to the particular transverse width of the condensate $w\sim 1\lambda_L$, as is shown in Fig. 1(b). Physically, this is due to the rapid oscillation of light-induced dipole radiation in space with the light wavelength λ_L. So far, we have a general understanding on the properties of spin coupling in the optical lattice. Now, it is time to examine the nonlinear dynamics of the spin waves. For the purpose of comparison, we consider three cases below: the NN approximation, the NNN approximation, and the long-range spin coupling, respectively.

B. Nearest-neighbor approximation

Although the spin dynamics in the lattice atomic spin chain is physically governed by the long-range spin coupling, it is certainly helpful to look at the nonlinear dynamics of spin waves under the near-neighbor approximations. First, we consider the nearest-neighbor (NN) approximation where the on-site spin is assumed to only couple to the spins at its two neighbor sites, and the longer range coupling is artificially cut off. Using the NN approximation in Eqs. (13)–(15), we have

$$M_{12}M_{21}\approx -(2\phi_0^2-4S)J_{01}^2(\cos Q-1)\times\cos q\left\{(4S-6\phi_0^2)\cos q\cos Q-(2\phi_0^2+4S)\cos q+4\phi_0^2\frac{J_{01}^z}{J_{01}}\cos Q\right\}. \tag{17}$$

From the criteria for the spin wave MI, $M_{12}M_{21}<0$, and the condition $2S\gg\phi_0^2$, we obtain the condition for the spin wave MI,

$$\left\{(4S-6\phi_0^2)\cos q\cos Q-(2\phi_0^2+4S)\cos q+4\phi_0^2\frac{J_{01}^z}{J_{01}}\cos Q\right\}\cos q>0. \tag{18}$$

For the long wavelength modulation $Q\ll 1$, Eq. (18) can be simplified to

$$(\alpha_1-2\cos q)\cos q>0, \tag{19}$$

where $\alpha_1=J_{01}^z/J_{01}$ stands for the relative strength of the longitudinal spin coupling to the transverse one at the NN site. Equation (19) indicates that the long wavelength MI in the NN approximation is governed by the competition between the longitudinal spin coupling due to static magnetic dipole-dipole interaction and the transverse one due to light-induced dipole-dipole interaction.

For a blue-detuned optical lattice, the condensates are trapped at the standing-wave nodes where the laser intensity is approximately zero. As a result, the light-induced dipole-dipole interaction can be neglected. Then, we have an isotropic spin coupling due to the static magnetic dipole-dipole interaction. This leads to $\alpha_1=2$. Equation (19) becomes

$$(1-\cos q)\cos q > 0. \tag{20}$$

From Eq. (20), we can easily find that, when the wave number q of NCSW lies in the region $(\pi/2, 3\pi/2)$ including the boundary of Brillouin zone $(q=\pi)$, $M_{12}M_{21}>0$. This means, in this region, the NCSWs with only NN spin coupling are always stable for long wavelength modulation. Beyond this region, the MI of NCSWs occurs.

However, for a red-detuned optical lattice, the condensate atoms are trapped at the maxima of the standing-wave light intensity and the light-induced dipole-dipole interaction is dominant over the static magnetic dipole-dipole interaction. In such an anisotropic lattice, the competition between the longitudinal and transverse spin couplings leads to $\alpha_1 \ll 1$. As a result, the condition $M_{12}M_{21}>0$ is always satisfied for arbitrary spin wave number q. Hence, we conclude that in a red-detuned optical lattice, the NCSWs with only NN spin coupling are always stable under long wavelength modulation.

C. Next-nearest-neighbor approximation

Before going to study the long-range effect, in this section, we look at a case slightly beyond the NN approximation: the next-nearest-neighbor (NNN) approximation. In the NNN approximation, the on-site spin is coupled to the spins at its four near-neighbor sites. Again, under the long wavelength modulation $Q \ll 1$ and the condition $\phi_0^2 \ll 2S$, we obtain the following MI condition:

$$(\cos q + 4A_2 \cos 2q)(2\cos q + 2A_2 \cos 2q - \alpha_1 - A_2\alpha_2) < 0, \tag{21}$$

where $A_2 = J_{02}/J_{01}$ is the relative strength of transverse spin coupling at different sites, and the relative strength of the longitudinal to transverse spin coupling at the NN and NNN site is $\alpha_j = J_{0j}^z/J_{0j}$ $(j=1,2)$.

For a blue-detuned optical lattice, we have $\alpha_1=\alpha_2=2$. Equation (21) simply becomes

$$\cos q + 4A_2 \cos 2q > 0. \tag{22}$$

The occurrence of the MI depends on the spin wave number q and the relative transverse spin coupling strength A_2. A typical case is to look at the spin wave modes near the Brillouin zone boundary $(q=\pi)$. This leads to the simple MI criteria

$$1 - 4A_2 < 0. \tag{23}$$

In other word, when the relative transverse spin coupling strength $A_2 > 0.25$, $M_{12}M_{21}<0$, the MI of NCSWs would appear near the Brillouin zone boundary. Evidently, this result is totally different from that in the NN approximation. Similar case was discussed in Ref. 26, where they studied a one-dimensional ferromagnetic chain of N spins with the isotropic exchange interactions. Here, for the blue-detuned optical lattice, our case is just isotropic. This result indicates that the long-range spin coupling will completely change the dynamic of the NCSWs.

For a red-detuned optical lattice, we have $\alpha_1, \alpha_2 \ll 1$, and the MI condition is simplified as

$$(\cos q + 4A_2 \cos 2q)(\cos q + A_2 \cos 2q) < 0. \tag{24}$$

Similarly, for the spin wave modes near the Brillouin zone boundary $(q=\pi)$, Eq. (24) produces the result

$$(1-4A_2)(1-A_2) < 0, \tag{25}$$

and now the MI criteria become

$$0.25 < A_2 < 1. \tag{26}$$

We see that in the NNN approximation, the MI of NCSWs near the Brillouin zone boundary $(q=\pi)$ for both the blue-detuned optical lattice and the red-detuned one has the similar properties except that the MI criteria request an upper bound for the relative transverse spin coupling strength A_2 in the red-detuned case. Again, we find that the NNN spin coupling changes the nature of the MI of the NCSWs in the case with the NN approximation.

D. Long-range interaction

Now, we come to study the effects of the long-range spin coupling on the nonlinear spin wave dynamics by including the spin coupling at all sites through the whole optical lattice. First, for a qualitative analysis, we consider the MI of the NCSWs near the Brillouin zone boundary $(q=\pi)$. This leads to

$$M_{21}M_{12} = 8J_{01}^2S^2\sum_j A_j(-1)^j[\cos(Qj)-1]\sum_j A_j\{[2\alpha_j\beta^2 + 2(-1)^j - 3\beta^2(-1)^j]\cos(Qj) - (\beta^2+2)(-1)^j\}, \tag{27}$$

where we have set $\phi_0 = \beta\sqrt{S}$, and $A_j = J_{0j}/J_{01}(j=1,2,3,\ldots)$ stand for the transverse coupling strength between the jth site spin and the on-site spin. $\alpha_j = J_{0j}^z/J_{0j}(j=1,2,3,\ldots)$ describe the ratio of the longitudinal and the transverse spin couplings.

For a blue-detuned optical lattice, the condition $\alpha_1=\alpha_2=\cdots=\alpha_j=2$ is satisfied, and under long wavelength modulation $(Q \ll 1)$, we have the MI criterion

$$f_B(w) = \sum_j (-1)^{j+1} j^2 A_j = 1 - 4A_2 + 9A_3 - 16A_4 + \cdots < 0. \tag{28}$$

The summation in Eq. (28) contains different terms describing the long-range spin coupling for long wavelength modulation. It is very interesting that starting from the studied on-site spin (here we take as $j=0$), the terms from the even sites have a sign opposite to that from the odd sites in Eq. (28). The MI of the NCSW modes near the Brillouin zone boundary depends on the competition between the contribution of the even sites and that of the odd sites. When the contribution of the even sites is dominant, the NCSW modes are unstable; otherwise, they are stable.

In Fig. 2, the dependence of the MI of the NCSW modes near the Brillouin zone boundary on the transverse width of the BECs in a blue-detuned optical lattice is compared for the NNN approximation and the long-range spin coupling.

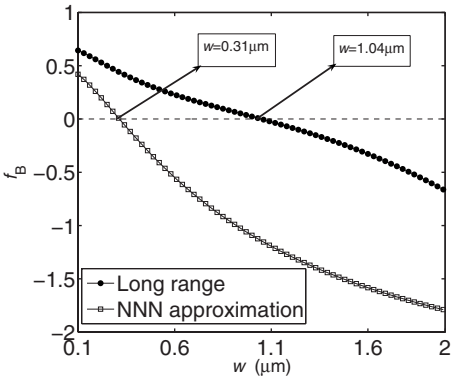

FIG. 2. The curve of function $f_B(w)$. The critical widths w for the MI to appear have been marked; the other parameters are chosen the same as in Fig. 1(a).

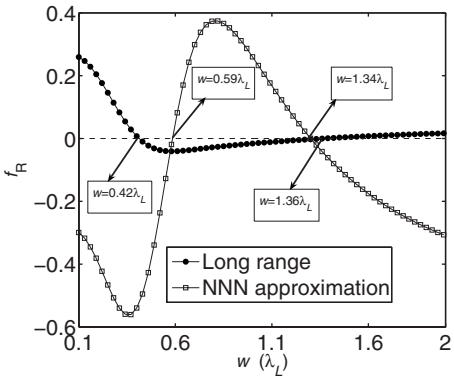

FIG. 3. The curve of function $f_R(w)$. The other parameters are chosen the same as in Fig. 1(b).

We find that in the NNN approximation, the stability requires a narrower range of transverse width than that in the long-range spin coupling. This can be easily understood. From Fig. 1(a), for the blue-detuned optical lattice, one can see that the relative strength of the transverse spin coupling due to static magnetic interaction, $A_j=J_{0j}/J_{01}=J_{0j}^z/J_{01}^z$, rapidly increases with the increase of the transverse width w. In the NNN approximation, the stability determined by Eq. (23) exists only for narrow transverse width w due to the rapidly rising spin coupling strength A_2 with w [see Fig. 1(a)]. However, for the long-range spin coupling, the stability depends on the competition of the spin coupling from all sites through the lattice. In particular, the contribution from the odd sites always cancels out that from the even sites. As a result, a larger range of transverse width w can be allowed for the stability in the long-range case. Although there is such a difference between the NNN approximation and the long-range spin coupling, from Fig. 2, we also see that the NNN approximation is reasonably good to describe the tendency of the MI of the NCSWs in a blue-detuned optical lattice where the spin coupling is isotropic.

For a red-detuned optical lattice, the situation changes dramatically due to the anisotropy of the spin coupling described by the relations $\alpha_1, \alpha_2, \ldots, \alpha_j \ll 1$. From Eq. (27), this leads to the MI criteria at the Brillouin zone boundary under the long wavelength modulation,

$$f_R(w) = \sum_j (-1)^{j+1} j^2 A_j \sum_j (-1)^{j+1} A_j$$
$$= (1 - 4A_2 + 9A_3 - 16A_4 + \cdots)(1 - A_2 + A_3 - A_4 + \cdots)$$
$$< 0. \quad (29)$$

Being different from the case of a blue-detuned optical lattice, an additional modulation $(1-A_2+A_3-A_4+\cdots)$ appears in the MI criteria due to the anisotropy of spin coupling in a red-detuned optical lattice. Again, in Fig. 3, we compare the dependence of the MI of the NCSW modes near the Brillouin zone boundary on the transverse width of the BECs for the NNN approximation and the long-range case. We find that the NNN approximation is completely invalid to describe the spin dynamics in a red-detuned optical lattice where the long-range anisotropic spin coupling exists. In particular, we see that the NNN approximation predicts a stable region in the range of transverse width of BECs around the light wavelength λ_L, but the case with the long-range spin coupling exhibits instability in this region. This is also consistent with calculation of the relative spin coupling strength given in Fig. 1(b), where the coefficients $A_j=J_{0j}/J_{01}$ rise up when the transverse width of the BECs $w \sim 1\lambda_L$ due to the light-induced dipole-dipole interaction.

Finally, we look at the general case by numerically working out the MI region in terms of Eq. (13)–(16). The MI regions of nonlinear spin wave in (Q,q) plane are shown in Figs. 4 and 5, which correspond to the blue-detuned and the red-detuned optical lattice, respectively. In these figures, the black zone marks the unstable regions in which the amplitude of any perturbation wave would exhibit a rapidly exponential growth with time, and the rest areas (blank regions) are the stable regions. For comparison, we also show the MI regions for the cases of the NN and NNN approximation in Fig. 4. In the NN approximation, the MI regions do not depend on the change of the transverse width of the condensates. In the NNN approximation and the long-range case, the MI regions change gradually with the increase of the transverse width of the condensates. After the transverse width w exceeds a certain value, the MI appears near the Brillouin zone boundary. This is consistent with our qualitative analysis given above. In addition, we see that the MI regions mainly distribute around the long wavelength modulation in the blue-detuned optical lattice.

In the red-detuned optical lattice, our calculation shows that the NCSWs are always stable under the NN approximation. This further extends the conclusion derived in Sec. III B to arbitrary modulation. In the NNN approximation, the unstable regions appear near the Brillouin zone boundary for either narrow or wider condensate. However, these regions shrink and even disappear while the long-range interaction takes effect. In particular, the MI of NCSW modes near the Brillouin zone boundary in the case of the long-range spin coupling is enhanced for the width around the wavelength of light due to the light-induced dipole-dipole interaction. Hence, again, we see that the NNN approximation completely fails to describe the spin dynamics in the red-detuned optical lattice where the anisotropic long-range spin coupling

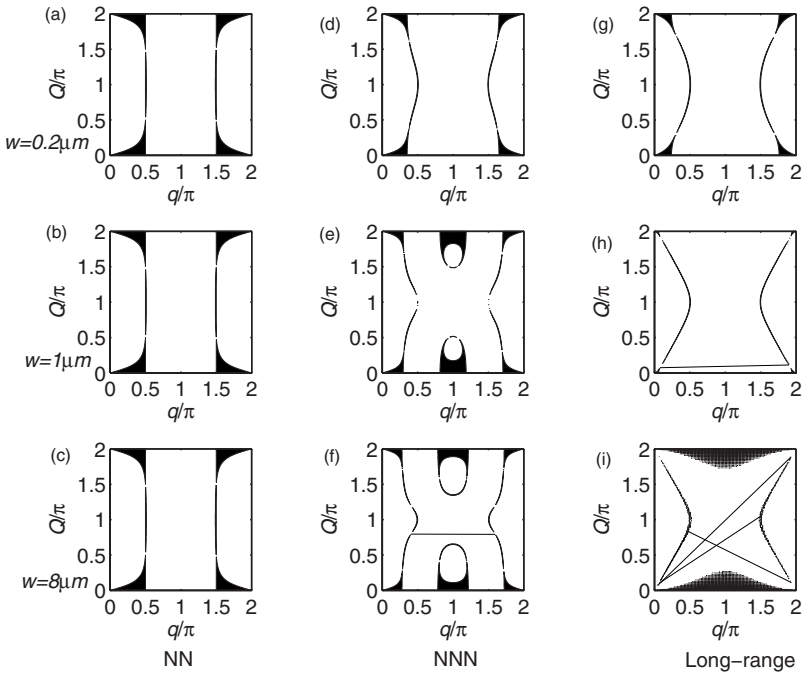

FIG. 4. Plots of the MI regions in the blue-detuned optical lattice. We have used a total number of 200 lattice sites with 2000 atoms in each site, and the amplitude of spin wave $\phi_0=0.25\sqrt{S}$.

caused by light-induced dipole-dipole interaction plays a central role in the spin dynamics.

IV. NUMERICAL SIMULATION

In Sec. III, our results are based on the theory of linear stability analysis. However, we know that the linear stability analysis is limited because it can only predict the onset of instability and does not tell us anything about the long-time dynamical behavior of the system when the instability grows.[16,27] To further confirm that our linear instability analysis given above can correctly describe the initial stage of instability in the atomic spin chain, we exactly solve the set of coupled nonlinear differential equations [Eq. (6)] by numerical fourth-order Runge-Kutta algorithm. The numerical simulation cannot only confirm the analytical prediction given in Sec. III for short time but it can also give the long-time spin dynamics of the nonlinear system.

Here, we consider a case of an atomic spin chain of 100 sites with periodic boundary conditions in a red-detuned optical lattice as an example for our numerical simulation. The initial conditions of the atomic spin chain at $t=0$ are assumed to have the form

$$\psi_n(0) = [\phi_0 + \eta\cos(nQ)]\cos(nq) + i[\phi_0 + \eta\cos(nQ)]\sin(nq), \tag{30}$$

where ϕ_0 is the amplitude of the plane spin wave and the modulation amplitude $\eta \ll \phi_0$. In our simulation, the amplitude of the modulated plane spin wave is taken to be $\phi_0 = 0.25\sqrt{S}$, the wave numbers q and Q are chosen in the form $q=2\pi k/N$ and $Q=2\pi K/N$, where k and K are integers, and $N=100$. In order to monitor the time evolution of individual Fourier components, we employ spatial Fourier transform of the wave function,

$$m(p,t) = \sum_{n=0}^{N-1} \psi_n(t) e^{i(2\pi np/N)}, \tag{31}$$

where $0 \leqslant p < N$. According to Figs. 3 and 5, when $w=1\lambda_L$, the MI can occur as the extended wave vector nearby $q=\pi$, i.e., near the Brillouin zone boundary with small modulational wave vector Q. To show the long-time spin dynamical

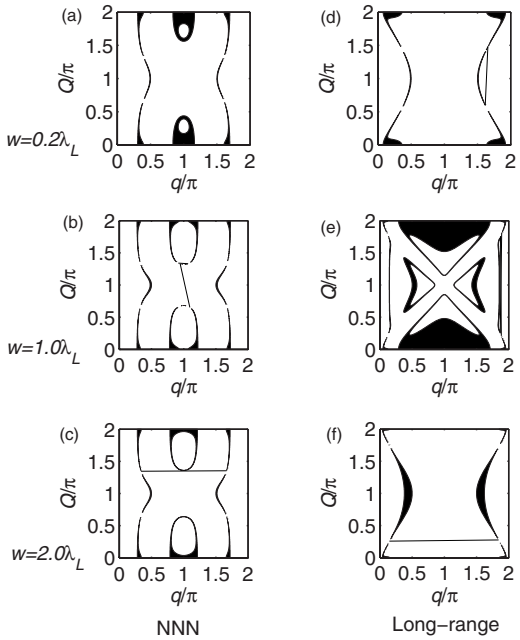

FIG. 5. Plots of MI regions in the red-detuned optical lattice. The other parameters are chosen the same as in Figs. 1(b) and 4. The plots of stable regions for the case of the NN approximation are not displayed here.

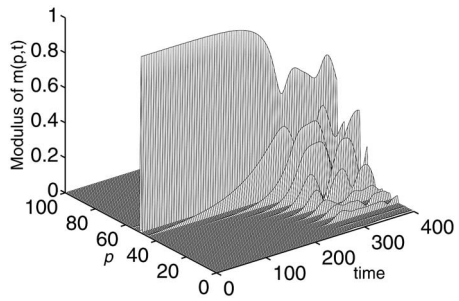

FIG. 6. Long-time evolution of nonlinear modulation waves in the optical lattice. Initially, the plane spin wave with $q=50\pi/50$ with amplitude $\phi_0=0.25\sqrt{S}$ and the perturbation vector $Q=5\pi/50$ with amplitude $\eta=0.005\phi_0$. Amplitudes are shown in relative units and time is measured in units of periods T. The other parameters are chosen the same as in Fig. 5.

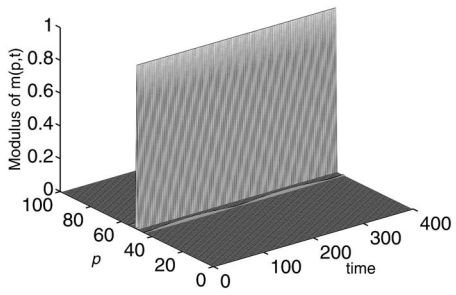

FIG. 7. The long-time evolution of a stable nonlinear spin wave. The parameters are same as in Fig. 6, but for $w=2\lambda_L$.

behavior in this region, we choose the extended wave having a wave vector $q=50\pi/50$ and the small-amplitude modulational waves having a wave vector $Q=5\pi/50$.

The long-time evolution of the complete Fourier spectrum is shown in Fig. 6, where the time step T denotes the period of the spin wave that can be derived from the frequency given in the dispersion relation of Eq. (8). From Fig. 5, the extended wave is unstable. We observe the corresponding growth of the satellite sidebands in Fig. 6 with time, and the sidebands $q\pm Q$, $q\pm 2Q$, $q\pm 3Q$, …, grow one by one. For the transverse width $w=2\lambda_L$, the same modulated plane wave will be stable from Fig. 5, and its long-time evolution shown in Fig. 7 confirms the result.

From Fig. 7, we see that there is no satellite sideband displaying any exponential growth, even though there exist other harmonics that have a very small amplitude for a long time. The same verifications of the stability of spin waves in other regions based upon the result of linear stability analysis can also be done with the same time scale and physical parameters. The results of numerical simulation have demonstrated that the linear stability analysis presented in Sec. III can effectively describes the initial stage of instability of NCSW in atomic spin chain. The numerical simulation also shows that the discrete atomic chain of spinor BECs can support long-lived excitations in the presence of small-amplitude modulation with suitable wave numbers. Furthermore, it is also possible for us to generate strong localized long-lived spin excitations in this discrete chain by using the nature of nonlinear instability.

V. CONCLUSION

In conclusion, the MI of the nonlinear coherent spin waves in spinor BECs confined in an optical lattice is studied. By using the methods of HP transformation and the linear stability analysis, the MI criteria subject to the long-range dipole-dipole interaction are obtained analytically. Based on the analytic results, the properties of the MI of the NCSW modes near the Brillouin zone boundary under the long wavelength modulation are revealed for both a blue-detuned and a red-detuned optical lattice, respectively. For a blue-detuned optical lattice, the static magnetic dipole-dipole interaction dominantly determines the spin wave dynamics. In this case, the spin coupling is isotropic. The instability occurs for wider BECs, and the NNN approximation is reasonably good to describe the MI of the NCSW modes near the Brillouin zone boundary even the long-range spin coupling exists. For a red-detuned optical lattice, the anisotropic long-range spin coupling caused by the light-induced dipole-dipole interaction plays a central role in the spin dynamics. As a result, the instability occurs strongly for BECs with width near the light wavelength λ_L. The NNN approximation fails to describe the spin dynamics due to the anisotropy and the long-range spin coupling. In general, compared to the conventional spin chain in solid-state magnetic materials, the atomic spin chain created in an optical lattice provides an ideal and powerful tool to study spin dynamics in a controllable way.

ACKNOWLEDGMENTS

This work was supported by the National Natural Science Foundation of China under Grants No. 10474055, No. 10588402, and No. 10447004, the National Basic Research Program of China (973 Program) under Grant No. 2006CB921104, the Science and Technology Commission of Shanghai Municipality under Grants No. 05PJ14038, No. 06JC14026, and No. 04DZ14009, and the Post Doctoral Fund of China (No. 44020570).

*Author to whom correspondence should be addressed; wpzhang@phy.ecnu.edu.cn

[1] J. Stenger, S. Inouye, D. M. Stamper-Kurn, H.-J. Miesner, A. P. Chikkatur, and W. Ketterle, Nature (London) **396**, 345 (1998).

[2] H. J. Miesner, D. M. Stamper-Kurn, J. Stenger, S. Inouye, A. P. Chikkatur, and W. Ketterle, Phys. Rev. Lett. **82**, 2228 (1999).

[3] D. M. Stamper-Kurn, H. J. Miesner, A. P. Chikkatur, S. Inouye, J. Stenger, and W. Ketterle, Phys. Rev. Lett. **83**, 661 (1999).

[4] M. S. Chang, C. D. Hamley, M. D. Barrett, J. A. Sauer, K. M. Fortier, W. Zhang, L. You, and M. S. Chapman, Phys. Rev. Lett. **92**, 140403 (2004).
[5] A. E. Leanhardt, Y. Shin, D. Kielpinski, D. E. Pritchard, and W. Ketterle, Phys. Rev. Lett. **90**, 140403 (2003).
[6] M. S. Chang, Q. Qin, W. Z. Zhang, L. You, and M. S. Chapman, Nat. Phys. **1**, 111 (2005).
[7] Nichilas P. Robins, Weiping Zhang, Elena A. Ostrovskaya, and Yuri S. Kivshar, Phys. Rev. A **64**, 021601(R) (2001).
[8] Lu Li, Zaidong Li, Boris A. Malomed, Dumitru Mihalache, and W. M. Liu, Phys. Rev. A **72**, 033611 (2005).
[9] J. Ieda, T. Miyakawa, and M. Wadati, Phys. Rev. Lett. **93**, 194102 (2004).
[10] W. Zhang, Han Pu, C. Search, and P. Meystre, Phys. Rev. Lett. **88**, 060401 (2002).
[11] H. Pu, W. Zhang, and P. Meystre, Phys. Rev. Lett. **87**, 140405 (2001).
[12] David Carpentier and Leon Balents, Phys. Rev. B **65**, 024427 (2001).
[13] V. Yu. Irkhin and M. I. Katsnelson, Phys. Rev. B **56**, 8109 (1997).
[14] L. J. Azevedo, A. Narath, Peter M. Richards, and Z. G. Soos, Phys. Rev. Lett. **43**, 875 (1979).
[15] R. Lai and A. J. Sievers, Phys. Rev. B **57**, 3433 (1998).
[16] Jean-Pierre Nguenang, Michel Peyrard, Aurelien J. Kenfack, and Timoleon C. Kofane, J. Phys.: Condens. Matter **17**, 3083 (2005).
[17] I. Daumont, T. Dauxois, and M. Peyrard, Nonlinearity **10**, 617 (1997).
[18] V. M. Burlakov and S. A. Kiselev, Sov. Phys. JETP **72**, 854 (1991).
[19] Y. S. Kivshar and M. Salerno, Phys. Rev. E **49**, 3543 (1994).
[20] K. W. Sandusky and J. B. Page, Phys. Rev. B **50**, 866 (1994).
[21] Kevin Gross, Chris P. Search, Han Pu, Weiping Zhang, and Pierre Meystre, Phys. Rev. A **66**, 033603 (2002).
[22] J. Javanainen, Phys. Rev. Lett. **72**, 2375 (1994).
[23] J. Callaway, *Quantum Theory of the Solid State* (Academic, New York, 1991).
[24] W. M. Zhang, D. H. Feng, and R. Glimore, Rev. Mod. Phys. **62**, 867 (1991).
[25] Axel Griesmaier, Jőrg Werner, Sven Hensler, Jűrgen Stuhler, and Tilman Pfau, Phys. Rev. Lett. **94**, 160401 (2005).
[26] R. Lai, S. A. Kiselev, and A. J. Sievers, Phys. Rev. B **56**, 5345 (1997).
[27] J. Ford, Phys. Rep. **213**, 271 (1992).